Integrated Nano, 2026, Vol. X, Iss. X, 111-121

DOI: 10.62184/in.jin010420264

Review Article

SCIENCE PARK PUBLISHER

Integrated Nano

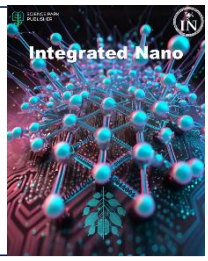

Integrated nanofiber membranes for green hydrogen production via water electrolysis

Ayah Dahash[1*], Adham H. Ibrahim[2], Mahmoud Amer[2]

[1]Foundation Department, Kuwait College of Science and Technology, Kuwait

[2]Mechanical Engineering Department, Faculty of Engineering, Alexandria University, Egypt

Received: 12, 04, 2026; Accepted: 18, 09, 2026; Published: 25, 11, 2026

© 2026 The Authors. Published by Science Park Publisher. This is an open access article under the CC BY 4.0 license (https://creativecommons.org/licenses/by/4.0/)

Abstract

This review examines the integration of electrospun nanofiber architectures into PEM and AEM water electrolyzers. It focuses on representative studies in which nanofibers are used in reinforced membranes, catalyst-layer architectures, or transport interlayers. Across these applications, nanofiber networks have mainly been explored to improve mechanical stability, swelling control, gas crossover, catalyst utilization, and water or gas transport. The reviewed studies show that nanofiber integration can support thin membrane design and porous electrode engineering, but the reported benefits are still difficult to compare directly because testing conditions and performance metrics vary widely. Key remaining challenges include defect-free scale-up, long-term durability under realistic operating conditions, and more consistent benchmarking across studies.

Keywords: Water electrolysis; Electrospinning; Nanofiber; PEM electrolyzer; AEM electrolyzer; Reinforced composite membranes; Catalyst layers

1. Introduction

Green hydrogen produced using renewable electricity is a promising route to decarbonize energy systems. Water electrolysis is a key technology because it converts electrical energy into hydrogen through the electrochemical splitting of water. Further technological advancements are still required to improve electrolyzer efficiency, durability, and long-term performance [1]. Practical deployment also remains limited by cost and by performance losses associated with catalysts, membranes, interfaces, and two-phase transport. Electrospinning enables the fabrication of nanofiber mats with controllable fiber diameter, porosity, composition, and network structure [2]. These characteristics make nanofiber architectures attractive for electrolyzer components because they can provide mechanical reinforcement, high-surface-area catalyst structures, and tailored pathways for ionic, water, and gas transport.

Water electrolysis splits liquid water into hydrogen and oxygen through two coupled electrochemical half-reactions. The hydrogen evolution reaction (HER) occurs at the cathode, while the oxygen evolution reaction (OER) occurs at the anode. In PEM water electrolyzers, protons (H^+) are transported through the membrane from the anode to the cathode, whereas hydroxide ions (OH^-) are the main charge carriers in AEM water electrolyzers. HER on Pt in acidic PEM environments is generally fast and contributes relatively small activation losses, whereas HER in alkaline/AEM environments is slower because water dissociation is required and the local electrolyte environment affects the reaction kinetics [3]. In contrast, OER is kinetically slower and often contributes substantially to

Integrated Nano, 2026, Vol. X, Iss. X, 111-121
DOI: 10.62184/in.jin010420264

activation losses. Gas-bubble formation, water transport, membrane hydration, and ionic resistance can introduce additional mass transport and ohmic losses [4]. Consequently, practical electrolyzers require an applied voltage above the thermodynamic minimum to overcome kinetic, resistive, and transport limitations.

This review focuses on the integration of nanofiber architectures, with particular emphasis on electrospun structures, into PEM and AEM water electrolyzers. It examines their use in reinforced membranes, catalyst layers, and electrocatalyst structures, as well as porous transport layers or functional interlayers. Particular attention is given to the relationships between nanofiber architecture and electrolyzer-relevant properties, including ionic conductivity, mechanical and dimensional stability, gas crossover, catalyst utilization, and water and gas transport. Recent reviews have primarily addressed electrospun nanofibers from an electrocatalyst perspective, focusing on HER and OER activity, catalyst composition, and structural or electronic modification [5, 6]. Broader reviews of ordered membrane-electrode assemblies have considered multiple electrolyzer components, including membranes, catalyst layers, and porous transport layers, without specifically focusing on nanofiber-based integration [7]. In contrast, the present review adopts a nanofiber-specific, cross-component perspective by examining how these architectures are incorporated across membranes, catalyst layers, and transport structures in both PEM and AEM water electrolyzers. This approach allows the structural strategies, quantitative performance outcomes, durability limitations, and practical integration challenges reported across studies to be considered together from an electrolyzer-focused perspective. The overall methodology used to identify, classify, and compare the selected studies is summarized in Figure 1.

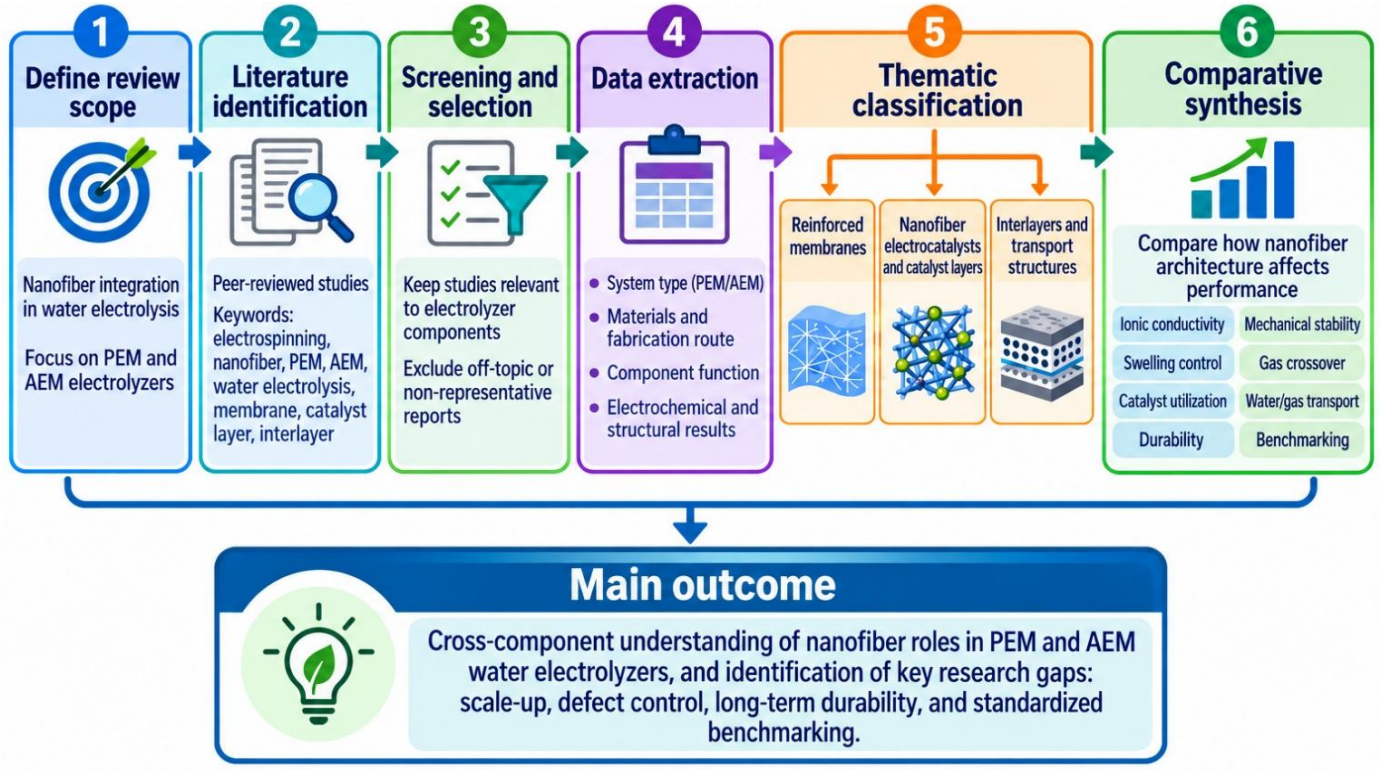

Figure 1. Review methodology used for the identification, classification, and comparative analysis of nanofiber-based approaches in PEM and AEM water electrolyzers.

Integrated Nano, 2026, Vol. X, Iss. X, 111-121
DOI: 10.62184/in.jin010420264

Review Article

2. Common water electrolysis techniques

2.1. PEM water electrolysis

This system uses a proton-conducting polymer electrolyte (most commonly perfluorosulfonic acid (PFSA)-type membranes) and runs in a strongly acidic environment, so protons (H^+) are the charge carriers migrating through the membrane from anode to cathode (Figure 2).

This architecture enables a compact zero-gap membrane electrode assembly (MEA) arrangement with very low ionic resistance. As a result, PEM stacks can reach high current operation and deliver high-purity hydrogen, even under differential-pressure conditions that allow direct production of pressurized H_2. At the anode, water is supplied through a porous transport layer (PTL) and catalyst layer, where it is oxidized to O_2; at the cathode, protons and electrons recombine to form H_2. Because the membrane must remain fully hydrated to maintain high proton conductivity, PEM performance is extremely sensitive to water management. Insufficient water feed or local dry-out (water starvation) sharply increases membrane resistance, which raises the cell voltage and can trigger severe thermal and mechanical damage. The porous layers (PTL and catalyst layer) therefore play a dual role, uniformly distributing liquid water to the active sites and rapidly removing oxygen bubbles so the anode does not become mass-transport-limited. PTL structure, wettability, and porosity are known to control water and gas pathways and are a major lever for limiting oxygen blocking and ohmic losses in acidic PEM water electrolysis (PEMWE) operation [3]. In addition, MEA microstructure factors such as ionomer content and local hydration within the anode catalyst layer strongly affect reaction kinetics and transport at elevated temperature, so optimization of these parameters is essential for stable, high-current PEM operation [8].

2.2. AEM water electrolysis

This system uses an anion-conducting membrane and works under alkaline conditions, meaning hydroxide ions (OH^-) are the mobile charge carriers travelling from cathode to anode (Figure 2). In principle, this allows the use of earth-abundant HER/OER catalysts and cheaper metallic hardware because the environment is not acidic. This makes AEM water electrolysis (AEMWE) an attractive lower-cost route compared with PEM. Recent single-cell demonstrations show that, when the catalyst layers and anion-exchange ionomer (AEI) binders are well-engineered, AEM electrolyzers can achieve high current operation with non-precious catalyst families such as Ni-, Fe-, or Co-based materials, narrowing the performance gap to PEM [9]. However, durability is still the key bottleneck. The anode region experiences very high oxidative potentials and oxygen-rich conditions. The most widely observed failure mode in modern AEMWE is chemical oxidation of the anode ionomer and sometimes adjacent membrane, which gradually reduces OH^- conductivity, weakens catalyst-layer cohesion, and accelerates voltage rise during long-term operation. This explains why many devices still rely on added alkaline electrolyte or protective design features to sustain stability.

2.3. Key current bottlenecks motivating nanofiber membranes integration

Despite strong progress, both PEM and AEM water electrolyzers still face material and transport limits that become severe at industrial current densities. In PEM electrolysis, operation above 2-3 $A.cm^{-2}$ often triggers mass-transport losses. Oxygen bubbles accumulate in the anode porous transport and catalyst layers and restrict liquid-water access, while insufficient local hydration causes membrane dry-out and performance instability under high load [10]. At the same time, PEM systems depend on Ir-based anode catalysts, and primary cell studies show that maintaining high OER activity with much lower Ir loading is essential yet challenging, making catalyst cost a persistent scale-up barrier [11].

Durability is another bottleneck. Thinner membranes reduce ohmic loss but increase H_2/O_2 crossover, which promotes peroxide formation and chemical attack on the membrane and catalyst interfaces and raises safety concerns, especially under differential-pressure operation [12]. In AEM electrolysis, the intended cost advantage is limited by electrochemical instability of anode ionomers and membranes in locally alkaline, high-potential OER environments, leading to voltage rise and decay in pure-water or low-alkali operation [13]. Under the high oxidative potential of the AEMWE anode, ionomer degradation can proceed through direct electrochemical oxidation and radical-mediated pathways.

Integrated Nano, 2026, Vol. X, Iss. X, 111-121
DOI: 10.62184/in.jin010420264

Review Article

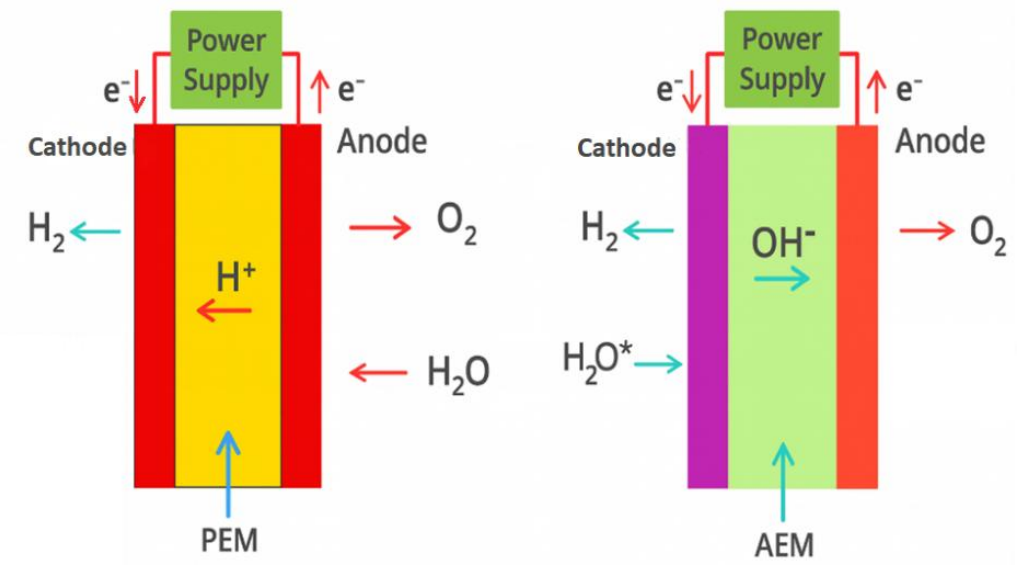

Figure 2. Operating principle of PEM (left) and AEM (right) water electrolyzers. For PEM, water is fed to the anode, protons (H^+) cross the membrane to the cathode and form H_2, and O_2 is released at the anode. For AEM, water feed (often with added alkaline electrolyte in many current demonstrations) (H_2O^*) is supplied, hydroxide ions (OH^-) move from the cathode to the anode, H_2 is produced at the cathode, and O_2 at the anode.

Hydroxyl radicals can attack the cationic groups and the polymer backbone. This attack can cause hydrogen abstraction, demethylation, and N–C bond cleavage in the cationic groups [13, 14]. Oxidation of the aromatic backbone can also lead to ring opening and polymer-chain scission [14]. These chemical changes reduce the integrity of the ion-conducting structure, impair OH^- transport, and increase ionic and ohmic resistance, which contributes to cell-voltage rise [13]. These problems are mainly related to transport, interface stability, and mechanical strength in the membrane and catalyst layers, which is why electrospun nanofiber networks are increasingly explored. They can create high-surface-area, well-connected porous pathways for water and gas transport, provide continuous charge-transport scaffolds, and mechanically stabilize thin membranes and catalyst layers.

3. Integration pathways of nanofiber in membranes

3.1. Electrospun scaffold concept

In this approach, a porous nanofiber mat is first made by electrospinning a mechanically robust polymer (Figure 3). The mat works as a three-dimensional scaffold. The ion-conducting polymer (PFSA for PEM, or quaternized polymers for AEM) is then cast or pore-filled into the mat. The final membrane becomes dense, gas-tight, and conductive, while the nanofiber network remains as an internal reinforcement. This structure separates two competing needs by providing high ionic conductivity from the ionomer phase and mechanical/dimensional stability from the nanofiber phase [15, 16].

3.2. Effects on conductivity, mechanical stability, and gas crossover

Electrospun nanofiber reinforcement is widely used to address a key practical constraint in electrolyzer membranes. Membranes are often pushed toward being thin to minimize ohmic losses, but thinning can compromise mechanical robustness and dimensional stability during hydration and thermal cycling. Introducing a nanofiber scaffold provides a continuous supporting framework that can stabilize the membrane structure while preserving the ion-conducting phase. Depending on the scaffold chemistry and how it is integrated (embedded, pore-filled, compressed, or chemically linked), reinforcement can target different performance needs, such as retaining conductivity under challenging humidity conditions, limiting swelling and void formation, and improving mechanical metrics. In some studies, reinforcement

Integrated Nano, 2026, Vol. X, Iss. X, 111-121
DOI: 10.62184/in.jin010420264

is also evaluated for its impact on gas transport, particularly hydrogen crossover when measured under a defined differential pressure.

Table 1 highlights two complementary PEM water electrolyzer (PEMWE) reinforcement logics. Inert nanofiber scaffolds, exemplified by an electrospun polysulfone (PSU) fiber web embedded in short-side-chain PFSA (Aquivion®), act mainly as a mechanical and dimensional backbone. In that case, the reinforced PFSA showed cell I–V comparable to the neat PFSA, while dimensional and mechanical stability improved and H_2 crossover decreased when measured under a 0.25 MPa differential pressure [15].

In contrast, ion-conducting fiber frameworks are intended to make the fiber phase contribute directly to proton transport. An all-PFSA composite (PFSA fiber skeleton within a PFSA matrix) was reported to increase conductivity at low relative humidity (RH) (e.g., at 80°C and 40% RH) [17]. Similarly, a phytic-acid-doped PBI nanofiber framework that is infiltrated with Nafion was reported to improve low-humidity conductivity (e.g., at 80°C and 30% RH) while also showing lower water uptake and higher strength than Nafion in the reported metrics [18]. A hybrid pathway is also represented in the table. In this approach, dual-fiber electrospinning combines proton-conducting PFSA fibers with PVDF reinforcing fibers, together with a sulfonated-silica network formed inside the PFSA fibers, and this design was reported to increase conductivity across RH while reducing lateral swelling [19].

For AEM systems, Table 1 shows two scaffold-enabled approaches. One approach is covalent fiber–matrix linking, in which an electrospun PBI nanofiber mat pore filled with a bromomethylated mTPN precursor was cured to form covalent links and then quaternized, yielding conductivity of about 62 $mS \cdot cm^{-1}$, swelling reduced by about 37%, and AEMWE performance of about 1.98 V at 0.25 $A \cdot cm^{-2}$ (50°C, 1 M KOH) with stable membrane resistance for about 200 h [16]. A second approach is impregnation and pore-filling of an inert scaffold, in which a porous electrospun PSU scaffold was impregnated with a quaternary-ammonium ionomer to form a composite AEM. The table reports conductivity values for repeated Fu samples and notes mechanical improvements, including increases in Young's modulus and tensile strength. It also shows electrolyzer operation reaching a maximum current density of around 1001 $mA \cdot cm^{-2}$, maintained over 200 h [2].

Direct comparison between studies remains difficult because testing conditions are not consistent. Membrane conductivity and area-specific resistance (ASR) should be reported at clearly defined temperature and RH conditions. Gas crossover should be measured at a stated differential pressure and membrane thickness. For AEM systems, the electrolyte concentration should also be specified. Durability tests should report the current density, temperature, and operating conditions. Using more uniform testing protocols would make cross-study comparisons more reliable.

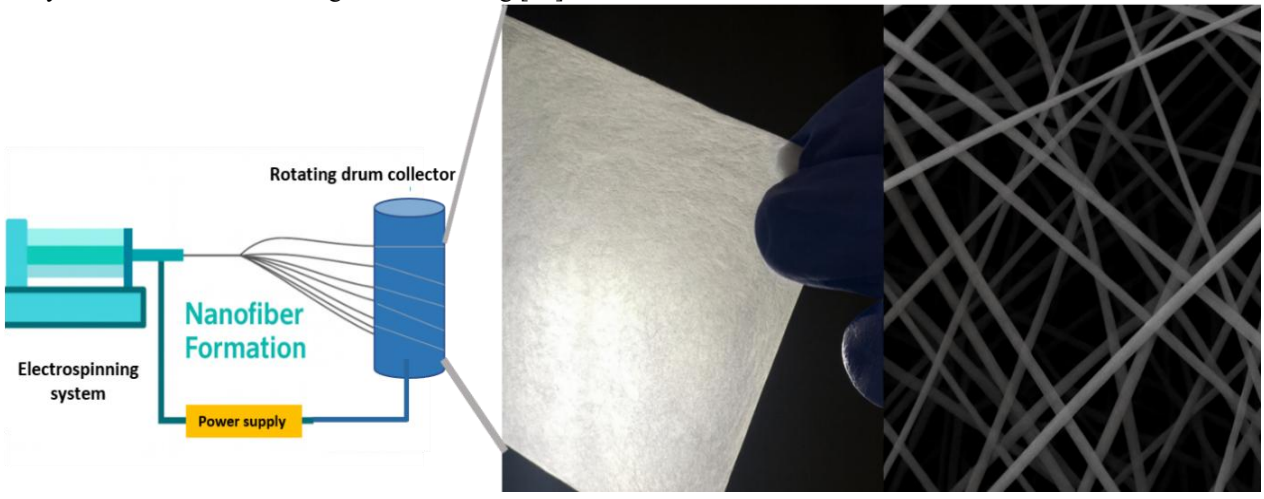

Figure 3. Electrospinning process and product: a rotating drum collector receives nanofiber from the electrospinning system (left), forming a flexible nanofiber mat (center) whose internal web-like fiber network is revealed in the scanning electron microscopy (SEM) image (right).

DOI: 10.62184/in.jin010420264

Review Article

Table 1. Representative nanofiber-reinforced membranes relevant to PEM and AEM water electrolysis.

System	Fabrication approach	Matrix / pore-filling ionomer	Advantages	Outcomes	Reference
PEM	Electrospun PSU nanofiber mat (approximately 5 wt%) embedded in Aquivion to form a reinforced PFSA membrane.	Short-side-chain PFSA Aquivion® (equivalent weight (EW) 830).	Adds a mechanical backbone with low H_2 permeability.	Cell I–V was similar to neat Aquivion, but H_2 crossover is reduced under 0.25 MPa differential pressure; dimensional and mechanical stability improved.	[15]
AEM	Electrospun PBI nanofiber mat pore-filled with a bromomethylated mTPN precursor, followed by curing to create covalent fiber–matrix bonding and quaternization to form the AEM.	mTPN (from bromomethylated precursor).	Stronger interface leads to lower swelling and voids and improved mechanical robustness while keeping conductivity.	Conductivity (σ) is about 62 mS.cm-1; swelling is reduced by about 37%; AEM water electrolysis shows a cell voltage of about 1.98 V at a current density of 0.25 $A \cdot cm^{-2}$ (50°C, 1 M KOH); membrane resistance remains stable for about 200 h.	[16]
PEM	All-PFSA composite membrane consisting of a blow-spun thin PFSA fiber framework embedded in a PFSA matrix, with 5–15 wt% ion-conducting fibers.	Aquivion PFSA matrix.	Increases continuous proton pathways without adding an inert phase.	Conductivity at 80°C, 40% relative humidity (RH) rises from 4.0 to 6.2 $mS.cm^{-1}$ (15 wt% fibers); high-RH conductivity slightly increased; slight tensile strength and elongation gains.	[17]
PEM	Electrospun and compressed phytic-acid-doped PBI nanofiber framework, subsequently infiltrated with Nafion to form a dense and continuous nanofiber network composite.	Nafion matrix (pore-filled).	Provides a strong scaffold and fast "surface proton conduction" along doped fibers.	Very low swelling and high strength: water uptake ~14% vs 34% Nafion, max stress 32.6 vs 11 MPa; improved low-humidity conductivity (4.2×10^{-3} $S.cm^{-1}$ at 80°C, 30% RH).	[18]
PEM	Dual-fiber electrospinning of PFSA nanofiber and PVDF reinforcing nanofiber, with a sulfonated silica network formed inside the PFSA fibers (Type-A).	PFSA matrix.	Boosts proton transport while PVDF limits swelling.	Best Type-A membrane shows 25–35% higher conductivity across RH range at 80°C, ~68% lower lateral swelling, and conductivity competitive with ultra-low-EW PFSA.	[19]

DOI: 10.62184/in.jin010420264

Table 1. Continued.

System	Fabrication approach	Matrix / pore-filling ionomer	Advantages	Outcomes	Reference
AEM	A porous electrospun PSU scaffold was prepared from 24 wt% PSU in NMP, then impregnated on both sides with Fumion® FAA-3 ionomer solution (redissolved in ethanol after precipitation from NMP using toluene) to form an anion-conducting membrane with reduced porosity and gas permeability.	Electrospun PSU nanofiber membrane.	Achieves ionic conductivity comparable to the Celgard-based reference composite AEM and is competitive in max current density.	Conductivity (σ): for repeated 15% Fu samples: S001 = 4.85 mS·cm^{-1}, S003 = 3.02 mS·cm^{-1} max current density 1001 mA·cm^{-2} maintained over 200 h. Young's modulus +128% to +260%, tensile strength +80% to +120%.	[2]

While Table 1 summarizes the broader performance of representative nanofiber-reinforced membranes, the effect of nanofiber loading on ionic resistance requires a more focused comparison. Ionically inert fibers can provide mechanical reinforcement but may reduce the fraction of the ion-conducting phase, whereas ion-conducting fibers can contribute directly to continuous transport pathways. Table 2 compares the available studies that relate nanofiber type and fraction to ionic conductivity and membrane resistance.

Table 2. Selected evidence on the effect of nanofiber type and fraction on ionic transport and membrane resistance.

Nanofiber type	Fiber fraction	Conductivity/resistance effect	Main interpretation	Reference
PSU, ionically inert	5 wt% ≈ 8 vol%	Through-plane conductivity decreased from 0.118 to 0.098 S.cm^{-1}; calculated membrane ASR increased from 0.038 to 0.046 Ω.cm^2.	Low inert-fiber loading introduces a modest resistance penalty while providing reinforcement.	[15]
PSU, ionically inert	18 wt%	In-plane conductivity at 80°C and 95% RH reached 0.14 S.cm^{-1}, about 22% below the non-reinforced membrane.	Higher inert-fiber loading increasingly dilutes the proton-conducting phase.	[15]
PFSA, ion-conducting	5, 10, 15 wt%	Through-plane conductivity at 80°C, 40% RH: 4.3, 5.0, and 6.2 mS.cm^{-1}, respectively; pristine PFSA = 4.0 mS.cm^{-1}.	Increasing the conductive-fiber fraction improves proton transport.	[17]
PVDF, ionically inert	15 wt%	Through-plane conductivity = 2.9 mS.cm^{-1} at 80°C, 90% RH.	At the same 15 wt% loading, inert fibers give much lower conductivity than conductive PFSA fibers.	[17]
Phy-doped PBI functional framework	≈11 and 24 vol%	The well-connected ≈24 vol% framework showed higher low-RH conductivity than the lower-fraction framework.	Fiber fraction can improve transport when continuous pathways form; poor pore filling can instead create voids.	[18]

Note: ASR values for the Giancola et al. membranes were calculated from the reported membrane thickness and through-plane conductivity using ASR = L/σ. Fiber fractions and conductivity values were reported under different experimental conditions; therefore, direct cross-study comparison should be made cautiously.

DOI: 10.62184/in.jin010420264

Table 2 shows a clear difference between inert and ion-conducting nanofibers. Increasing the amount of inert fibers can reduce ionic conductivity because they dilute the conducting phase. In contrast, ion-conducting fibers can improve proton transport when they form continuous pathways. However, fiber fraction alone is not sufficient, because connectivity and complete pore filling also affect membrane resistance.

3.3. Nanofiber electrocatalysts and catalyst layers

Electrospun nanofibers are increasingly explored as electrocatalysts or as structured catalyst layers in water electrolyzers because they naturally form a 3D porous, one-dimensional network. This network provides a high surface area with many exposed active sites and continuous electron pathways along the fiber direction. It also creates open channels for water supply and bubble removal. When transferred onto membranes or porous transport layers, nanofiber mats can widen the triple-phase reaction boundary (catalyst, ionomer, and water–gas), so higher performance is achieved at lower catalyst loading and with better durability.

3.3.1. Electrospun nanofiber catalysts for OER

In PEM electrolysis, the anode OER is the main kinetic and cost bottleneck because it must run in a strongly acidic environment. Ir-based oxides are the most established stable catalysts; RuO_2 is active but often less durable under acidic OER. Electrospinning offers a direct way to build a porous anode catalyst layer (ACL) from composite fibers containing catalyst particles and ionomer. Compared with conventional dense sprayed layers, the nanofiber ACL improves catalyst utilization and proton transport, enabling large reductions in noble-metal loading. Kovács et al. prepared electrospun IrOx nanofiber and varied the calcination temperature from 400 to 800°C. Structural evolution with temperature (oxidation state, crystallinity, and core–shell features) governed a clear activity–stability trade-off. Notably, fibers calcined around 500–600°C achieved higher specific activity at 1.60 V vs RHE and higher S-number stability than a commercial IrOx reference, showing that electrospinning can be used to engineer PEM-relevant OER catalysts [20]. Complementary to this materials-tuning approach, Hegge et al. combined electrospun IrOx nanofiber with a conventional IrOx nanoparticle anode, using the nanofiber network as a porous, conductive interlayer to improve electrical contact and maintain high porosity. In PEM water electrolyzer operation, the hybrid nanoparticle–nanofiber architecture improved catalyst utilization and stability compared with an identically loaded nanoparticle-only reference, illustrating how electrospinning can also be used as an electrode-engineering tool to address low-Ir anode limitations [21].

3.3.2. Nanofiber-based catalysts for HER

HER is faster than OER in PEM, but the cathode still benefits from porous, well-connected catalyst layers that avoid flooding and keep electronic contact. In AEM electrolysis (alkaline), HER becomes slower because it requires water dissociation; therefore, nanofiber architectures that expose more active sites and facilitate water access are especially attractive. Electrospinning enables self-supported HER mats or nanofiber-based catalyst inks with improved porosity and stability. Ahmed et al. synthesized a hydrated cobalt phosphate grown on commercially available carbon nanofiber ($Co_3(PO_4)_2{\cdot}8H_2O$/CNF) via a facile hydrothermal method, using CNF as a conductive scaffold. In 0.5 M H_2SO_4, the $Co_3(PO_4)_2{\cdot}8H_2O$/CNF composite showed improved HER activity and strong durability (including long-term cycling and 24 h operation) compared with $Co_3(PO_4)_2{\cdot}8H_2O$ or CNF alone, while Pt/C was used as a benchmark reference. The authors attribute the enhancement to higher electrochemically active surface area and faster charge transfer enabled by the conductive CNF-based composite structure [22]. In addition, Mukkavilli et al. synthesized electrospun 1D Ta_3N_5-(O) nanofiber by electrospinning a tantalum ethoxide/PVP precursor followed by NH_3 ammonolysis (800–1000°C), then evaluated HER activity in a half-cell and finally demonstrated device-level performance by employing the fibers as a cathode electrocatalyst in a PEM water electrolyzer, achieving 0.1 $A.cm^{-2}$ at 2 V with stable operation over 6 h [23]. These studies show different levels of device-level validation. The OER nanofiber interlayer reduced Ir loading from 1.2 to 0.2 mg Ir cm^{-2} while maintaining comparable cell performance. This represents an Ir-loading reduction of about 83%. In comparison, the Ta_3N_5-(O) HER electrode reached 0.1 $A.cm^{-2}$ at 2 V and was tested for 6 h. These results show the potential of nanofiber catalyst architectures, but longer and more consistent device-level testing is still needed.

3.4. Nanofiber interlayers and transport structures

Nanofiber structures can be introduced near the catalyst layer to support water transport, gas removal, and interfacial contact. Their high porosity and tunable fiber morphology make them attractive for transport-related functions in water electrolyzers. Fiber diameter, pore structure, wettability, and pathway connectivity can influence how easily water reaches the catalyst layer and how efficiently oxygen bubbles are removed.

In PEM water electrolyzers, this balance is important at high current density. Water must remain available at the anode while oxygen is removed efficiently from the reaction region. Poor transport can increase local mass-transport losses and reduce cell performance.

A direct PEMWE example is the work of Hegge et al., who inserted an IrO_x nanofiber mat between the titanium porous transport layer and a conventional IrO_x nanoparticle anode catalyst layer [21]. The nanofiber interlayer provided a porous and conductive structure that improved interfacial contact. With this hybrid architecture, the Ir loading was reduced from 1.2 to 0.2 mg Ir cm^{-2} while maintaining comparable cell performance. This corresponds to a reduction of more than 80%. The study shows that nanofiber interlayers can support catalyst utilization while also providing transport and interfacial benefits.

However, direct device-level evidence for nanofiber transport structures remains limited. More studies are needed to quantify their effects on water transport, gas removal, interfacial resistance, and long-term electrolyzer performance under comparable operating conditions.

4. Conclusion

This review examined how electrospun nanofiber architectures have been integrated into PEM and AEM water electrolyzers, with emphasis on reinforced membranes, catalyst-layer designs, and transport interlayers. The reviewed studies indicate that nanofiber integration can improve several component-level properties, including mechanical stability, swelling control, gas crossover, catalyst utilization, and water or gas transport. However, the reported benefits are still difficult to compare directly because the available studies use different materials, cell configurations, and performance metrics. At present, the main challenges are defect-controlled fabrication, long-term durability under realistic operating conditions, and the need for more consistent benchmarking against commercial electrolyzer components. Further progress will depend on studies that combine standardized electrochemical testing with careful structural and interfacial characterization.

Conflict of interest statement

The authors declare that they have no known competing financial interests or personal relationships that could have appeared to influence the work reported in this paper.

Funding

No funding was received for writing this manuscript.

Declaration of AI use in figure preparation

The authors used ChatGPT (OpenAI) to assist in the preparation of the schematic illustration presented in Figure 1. The figure was subsequently reviewed and edited by the authors to ensure scientific accuracy and consistency with the manuscript content. The authors take full responsibility for the final figure.

Author information

Corresponding author: Ayah Dahash*
E-mail: a.dahash@kcst.edu.kw
ORCID iD: 0009-0004-3189-6353

References

[1] Araujo, H. F., Gómez, J. A., & Santos, D. M. (2024). Proton-exchange membrane electrolysis for green hydrogen production: Fundamentals, cost breakdown, and strategies to minimize platinum-group metal content in hydrogen evolution reaction electrocatalysts. Catalysts, 14(12), 845. https://doi.org/10.3390/catal14120845

[2] Rakhshani, S., Araneo, R., Hein, L. A., Rinaldi, A., & Pozio, A. (2025). Fabrication and characterization of anionic composite membranes produced by electrospinning method. Polymers, 17(12), 1677. https://doi.org/10.3390/polym17121677

[3] Huang, B., Rao, R. R., You, S., Hpone Myint, K., Song, Y., Wang, Y., ... & Shao-Horn, Y. (2021). Cation- and pH-

dependent hydrogen evolution and oxidation reaction kinetics. JACS Au, 1(8), 1274–1287. https://doi.org/10.1021/jacsau.1c00281

[4] Ebbert, M. A., & Litster, S. (2024). Experimental assessment and analysis of mass transport limiting current density in water vapor-fed polymer electrolyte membrane electrolyzers. Scientific Reports, 14(1), 31637. https://doi.org/10.1038/s41598-024-79935-6

[5] Kang, Y., Hui, J., Wang, C., Gao, X., Zhao, Y., Qiao, Z., & Ding, C. (2025). Modulation of electrospun nanomaterials for boosting electrocatalytic water splitting. Journal of Electroanalytical Chemistry, 979, 118941. https://doi.org/10.1016/j.jelechem.2025.118941

[6] Cai, C. Y., Niu, W. J., Yu, B. X., Xu, L. Y., & Wang, F. M. (2026). Electrospun carbon nanofiber-based multifunctional electrocatalysts for zinc-air batteries and overall water splitting: Fabrication, progress, and perspective. Rare Metals, 45(3), e70127. https://doi.org/10.1002/rar2.70127

[7] Yu, L., Tian, B., Huang, W., Zhou, X., & Li, W. (2024). Advancements in ordered membrane electrode assembly (MEA) for water electrolysis. Current Opinion in Electrochemistry, 48, 101595. https://doi.org/10.1016/j.coelec.2024.101595

[8] Jang, Y., Seol, C., Kim, S. M., & Jang, S. (2022). Investigation of the correlation effects of catalyst loading and ionomer content in an anode electrode on the performance of polymer electrode membrane water electrolysis. International Journal of Hydrogen Energy, 47(42), 18229–18239. https://doi.org/10.1016/j.ijhydene.2022.04.019

[9] Zheng, Y., Ma, W., Serban, A., Allushi, A., & Hu, X. (2025). Anion exchange membrane water electrolysis at 10 A·cm^{-2} over 800 hours. Angewandte Chemie International Edition, 64(1), e202413698. https://doi.org/10.1002/anie.202413698

[10] Tao, Y., Wu, M., Hu, M., Xu, X., Abdullah, M. I., Shao, J., & Wang, H. (2024). High-performance porous transport layers for proton exchange membrane water electrolyzers. SusMat, 4(4), e230. https://doi.org/10.1002/sus2.230

[11] Chen, Y., Dai, C., Wu, Q., Li, H., Xi, S., Seow, J. Z. Y., ... & Xu, Z. J. (2025). Support-free iridium hydroxide for high-efficiency proton-exchange membrane water electrolysis. Nature Communications, 16(1), 2730. https://doi.org/10.1038/s41467-025-58019-7

[12] Tan, A., Song, J., Qiu, X., Liu, Z., Xia, L., Ju, C., ... & Liu, J. (2025). Catastrophic localized deflagration formation mechanisms and safety precautions in proton exchange membrane water electrolyzer. Nature Communications, 16(1), 9115. https://doi.org/10.1038/s41467-025-64162-y

[13] Jin, Y., Wu, B., Li, W., Wang, C., Fan, L., Wen, L., ... & Li, H. (2026). Oxidative stability as a guiding principle for durable ionomer cations in pure-water electrolysis. Nature Communications, 17, 1-10. https://doi.org/10.1038/s41467-026-73209-7

[14] Maxwell, D. S., Kendrick, I., & Mukerjee, S. (2024). Operando Raman spectroscopy reveals degradation byproducts from ionomer oxidation in anion exchange membrane water electrolyzers. Journal of the American Chemical Society, 146(32), 22431–22444. https://doi.org/10.1021/jacs.4c05721

[15] Giancola, S., Zatoń, M., Reyes-Carmona, Á., Dupont, M., Donnadio, A., Cavaliere, S., ... & Jones, D. J. (2019). Composite short side chain PFSA membranes for PEM water electrolysis. Journal of Membrane Science, 570, 69–76. https://doi.org/10.1016/j.memsci.2018.09.063

[16] Najibah, M., Tsoy, E., Khalid, H., Chen, Y., Li, Q., Bae, C., ... & Henkensmeier, D. (2021). PBI nanofiber mat-reinforced anion exchange membranes with covalently linked interfaces for use in water electrolysers. Journal of Membrane Science, 640, 119832. https://doi.org/10.1016/j.memsci.2021.119832

[17] Onuki, S., Kawai, Y., Masunaga, H., Ohta, N., Kikuchi, R., Ashizawa, M., ... & Matsumoto, H. (2024). All-perfluorosulfonated-ionomer composite membranes containing blow-spun fibers: Effect of a thin fiber framework on proton conductivity and mechanical properties. ACS Applied Materials & Interfaces, 16(8), 10682-10691. https://doi.org/10.1021/acsami.3c17643

[18] Wakiya, T., Tanaka, M., & Kawakami, H. (2021). Fabrication and electrolyte characterizations of nanofiber framework-based polymer composite membranes with continuous proton conductive pathways. Membranes, 11(2), 90. https://doi.org/10.3390/membranes11020090

[19] Santos, L. D., Powers, D., Wycisk, R., & Pintauro, P. N. (2020). Electrospun hybrid perfluorosulfonic acid/sulfonated silica composite membranes. Membranes, 10(10), 250. https://doi.org/10.3390/membranes10100250

DOI: 10.62184/in.jin010420264

[20] Kovács, M. M., Fritsch, B., Lahn, L., Bachmann, J., Kasian, O., Mayrhofer, K. J., ... & Dworschak, D. (2024). Electrospun iridium-based nanofiber catalysts for oxygen evolution reaction: Influence of calcination on activity–stability relation. ACS Applied Materials & Interfaces, 16(39), 52179. https://doi.org/10.1021/acsami.4c07831

[21] Hegge, F., Lombeck, F., Cruz Ortiz, E., Bohn, L., von Holst, M., Kroschel, M., ... & Vierrath, S. (2020). Efficient and stable low iridium loaded anodes for PEM water electrolysis made possible by nanofiber interlayers. ACS Applied Energy Materials, 3(9), 8219-8228. https://doi.org/10.1021/acsaem.0c00735

[22] Ahmed, I., Biswas, R., Sharma, R., Burman, V., & Haldar, K. K. (2023). Carbon nanofiber composite hydrated cobalt phosphate nanostructure as an efficient catalyst for hydrogen evolution reaction. Frontiers in Chemistry, 11, 1129133. https://doi.org/10.3389/fchem.2023.1129133

[23] Mukkavilli, R. S., Ichangi, A., Thiyagarajan, G. B., Vollnhals, F., Wilhelm, M., Bhardwaj, A., ... & Kumar, R. (2022). Electrospun 1D Ta_3N_5-(O) nanofibers as advanced electrocatalysts for hydrogen evolution reaction in proton exchange membrane water electrolyser. Open Ceramics, 10, 100267. https://doi.org/10.1016/j.oceram.2022.100267